JTTEE5 24:1506–1512
DOI: 10.1007/s11666-015-0331-2
1059-9630/$19.00 © ASM International

Mechanical and Microstructural Behavior of Cold-Sprayed Titanium- and Nickel-Based Coatings

P. Cavaliere and A. Silvello

(Submitted April 23, 2015; in revised form September 21, 2015)

Cold spraying is a coating technology that can deposit materials with unique properties. The coating forms through intensive plastic deformation of particles impacting on a substrate at temperature well below the melting point of the sprayed material. Recently, various studies have been published regarding the microstructural and mechanical evolution of metal-matrix composite coatings produced by cold spraying. Herein, we describe the principal results of the available literature in the field of cold-sprayed composites. It is shown that more research is required to solve various questions in this field, for example, the different deformation modes of the material exhibited for various processing conditions, the reinforcing percentage of different material combinations, and the mechanical properties resulting from these complex systems. In the present study, this issue is approached and described for cold-sprayed Ni- and Ti-based composites. Materials were produced with varying ceramic phase (BN and $TiAl_3$) fraction. The variation of the grain size, adhesion strength, porosity, and hardness of the deposits as a function of the ceramic phase fraction and processing parameters (impacting particle speed) is described. The interaction mechanisms between the cold-sprayed particles and the metal matrix during the coating process are presented and described. The results demonstrate a beneficial effect on grain size and porosity with increasing reinforcing phase percentage, as well as narrow processing parameter ranges to achieve the optimal properties with respect to the pure parent materials.

Keywords cold spraying, composites, mechanical properties, microstructure

1. Introduction

Cold spraying is a coating technology that can repair, restore, and protect bulk materials (Ref 1). It is based on severe plastic deformation occurring due to the impact of high-speed metallic and ceramic particles onto a substrate. The impacts occur at temperatures below the melting point of the sprayed material. Cold spraying can also be used to produce a highly innovative class of bulk materials characterized by properties that are not achievable by conventional metallurgical techniques (Ref 2, 3). Scientific research over the last 10 years has highlighted many interesting aspects of this innovative technology. However, many fundamental aspects remain to be clarified for effective application in aerospace, automobile, chemical industries, etc. The adhesion between the powder and the substrate is achieved in solid state, resulting in highly innovative and unique coating properties. The particles impact onto the substrate at high velocity, and deform and flatten through a severe plastic deformation mechanism, leading to micro and nano welding zones without particle melting. Such coating formation behavior cannot be achieved using conventional thermal spray-coating technologies. Cold spraying is designed to support many industrial applications, providing surface modification, wear resistance, thermal barriers, heat dissipation, restoration, sealing, rapid prototyping, esthetic coatings, fatigue resistance, and many other properties while avoiding the possible negative effects of high processing temperature or metallurgical differences among materials. Recently, great interest in the study of cold-sprayed metal–ceramic composites has been shown in the literature; such composites can be realized thanks to the possibility of depositing materials starting from very fine particles (from 10 to hundreds of nanometers) and tuning the final properties by modifying processing parameters, leading to severe plastic deformation. Various studies describing the microstructural and mechanical properties of cold-sprayed composite coatings have been published recently. The potential for preparing cold-sprayed nanostructured composites is well described in Ref 4-7. The authors show the potential of cold-spray composites for corrosion protection. These papers describe the possibility of producing composite coatings with different material combinations but fixed ceramic phase percentage. In Ref 8, 9, the authors describe the evolution of cold-sprayed composites with different ceramic phase percentages but employing narrow processing parameter ranges. In Ref 10-12, the authors describe the microstructural behavior of the deposited material when varying the reinforcing particle

P. Cavaliere and **A. Silvello**, Department of Innovation Engineering, University of Salento, 73100 Lecce, Italy. Contact e-mail: pasquale.cavaliere@unisalento.it.

dimensions. In these papers, the beneficial effects of the ceramic phase on grain refinement and adhesion strength are underlined. The effect of postspray heat treatment on the microstructural and mechanical properties of the deposit is well described in Ref 13, 14. The authors underline the stability of the composites up to very high temperatures, in this case with a ceramic volume fraction limited to 40%. The strengthening mechanisms acting in cold-sprayed composites are described in Ref 15. Here, the authors conclude that the main strengthening mechanisms in cold-spray coatings are work hardening, dispersion strengthening, and crystal refinement. The theoretically calculated hardness was in agreement with the experimental data. They demonstrate that work-hardening strengthening is the most significant mechanism, followed by the effect of crystal refinement and dispersion strengthening. In Ref 16, the authors present the wear and fracture toughness of cold-sprayed composites with up to intermediate percentages of ceramic phase, limited to 20%. This literature analysis shows that deeper research on the effects of both variation of the ceramic percentage and tuning of processing parameters is necessary to improve understanding of the deformation mechanisms involved during formation of composite coatings by cold spraying. This paper focuses on production of Ni- and Ti-based coatings with varying ceramic percentage between 0 and 50% using wide ranges of processing conditions, namely gas temperature and pressure and the consequent particle velocity at impact. The obtained mechanical and microstructural properties are described and analyzed as a function of both the processing parameters and the ceramic percentage. This study was performed to optimize the adhesion strength, refine the grains of the deposited material, and reduce its porosity. All the described properties are compared with those found by characterization of the pure base materials. This use of different ceramic volume fractions and various processing parameters (compatible with the sprayed powders) enables understanding of the different deformation mechanisms leading to the formation of cold-sprayed composite coatings.

2. Experimental Procedures

A CGT Kinetics 4000 series machine was used to realize cold-sprayed Ti- and NiCrAl-based coatings. The machine was equipped with a tungsten carbide De Laval nozzle with a rectangular throat cross-section of 2 mm × 4 mm and a 2 mm × 10 mm exit. Ti-6Al-4V was employed as the substrate for the Ti-based coatings, while IN718 was used as the substrate for the NiCrAl coatings. Ti-$TiAl_3$ and NiCrAl-BN mixtures, with varying percentage of $TiAl_3$ or BN in the range of 5 to 50%, were used. In all cases, ceramic–metal mixtures were employed as feedstock. The sprayed materials were obtained from previously prepared powder mixtures. Powders prepared via cryogenic ball milling were mixed in the requisite fractions before spraying. The mean starting particle dimensions were in the range of 30–60 μm. The cold-spraying parameters that were tuned in the present study were gas type, temperature, and pressure, and the nozzle–substrate distance, all of which influence the particle velocity. This aspect has been largely analyzed by Grujicic et al. (Ref 17), and the equations presented in that paper were used to calculate the particle impact velocity from the gas properties and nozzle geometry. The temperature was varied in the range of 25–600 °C, the pressure in the range of 0.5–4 MPa, and the nozzle–substrate distance in the range of 15–200 mm. The coating thickness was fixed at ~500 μm for all tested samples. The measured coating properties were the grain size, adhesion strength, and porosity of the deposit. The particle velocity was modified by varying the gas conditions and the nozzle–substrate distance. The composite properties were compared with those of pure feedstock with the same particle dimensions. The mean grain size of the deposits was measured by x-ray diffraction analysis using a Rigaku Ultima+ diffractometer based on Hall–Williamson plots. The porosity was calculated by statistical analysis (Ref 18) of scanning electron microscopy (SEM) observations (Zeiss EVO40); for each sample, five different images of 200 × 200 μm^2 were analyzed. The adhesion strength between the substrate and coating was determined according to the ASTM C633-01 standard (Ref 19).

3. Results and Discussion

Figure 1 shows the variation of the grain size of the deposit as a function of the reinforcing particle percentage for NiCrAl-BN and Ti-$TiAl_3$.

Both materials exhibited a decrease in grain size with increasing reinforcing percentage. The variation of the grain size of the deposits was narrower for higher reinforcement percentages. This effect is due to the enhanced deformation energy stored in the material, leading to more pronounced dynamic recrystallization with increasing ceramic phase content. The grain size of the deposits decreased with increasing ceramic phase percentage because the elastic energy transferred from the ceramic to the metallic particles during impact increases with increasing BN and $TiAl_3$ content. Naturally, these phenomena are more or less pronounced as a function of the different materials (metallic or ceramic). For NiCrAl-BN, strong sensitivity to the BN percentage is observed, while Ti-$TiAl_3$ shows a linear dependence on the ceramic phase percentage. In particular, for NiCrAl-BN, the efficiency of grain size reduction is strongly reduced for BN contents above 35%. For Ti-$TiAl_3$, a continuous dependence of the grain refinement effect on the $TiAl_3$ percentage is noted. In addition, the Ti-$TiAl_3$ composite shows narrower ranges of grain size compared with NiCrAl-BN. Many authors have related such behavior to the difference in melting and recrystallization temperatures of the materials impacting on the surface; this phenomenon influences the stress localization at the matrix–particle interface, playing a crucial role in the dynamic recrystallization occurring during the process. During impact, ceramic particles

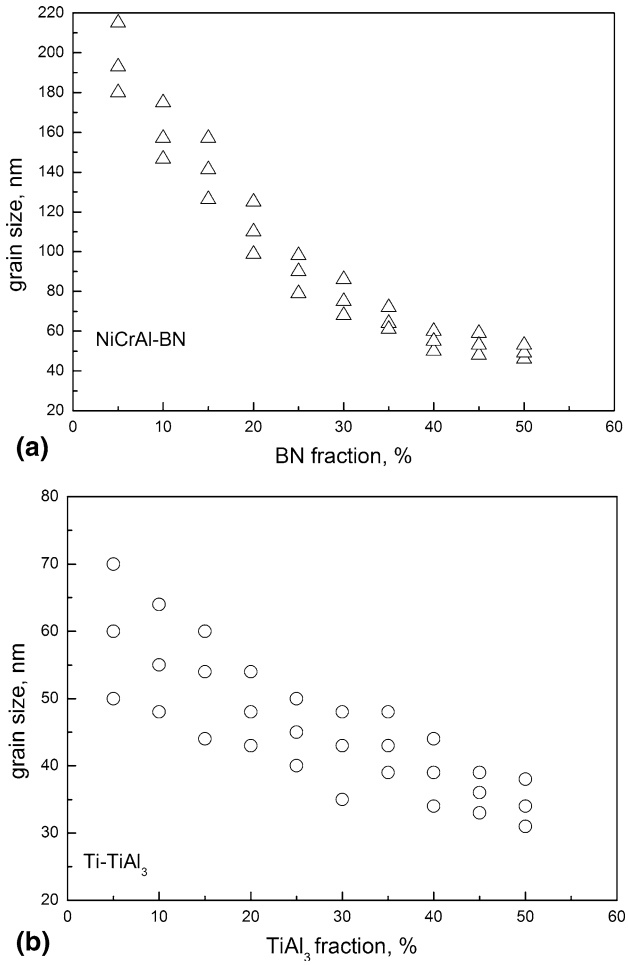

Fig. 1 Deposited grain size dimensions as a function of reinforcing phase percentage for NiCrAl-BN (a) and Ti-$TiAl_3$ (b)

deform elastically, transferring their kinetic energy to the metallic phase. The metallic matrix dissipates the transferred deformation energy through microstructural modifications (recovery, recrystallization, twinning, etc.). If the matrix cannot dissipate this energy, the ceramic particles fracture, leading to very different behavior from microstructural and mechanical points of view, also in the case of low reinforcing phase percentage (Ref 20). The main strengthening mechanism in such materials is, in fact, the effect of the ceramic particles on the grain refinement of the matrix at the nanoscale (Ref 21). This effect is also amplified by shot peening due to further impacting particles, normally leading to a variation of the coating density from the bulk to the surface. This effect can also be modified by changing the particle size of the ceramic phase (Ref 22). A crucial aspect when cold-spraying composites is to avoid melting after spraying, in order to guarantee crystallinity and obtain the best ceramic particle distribution in the matrix as well as uniform grain size. Should melting and resolidification of the material occur, dynamic recrystallization is absent and the resulting mechanical and microstructural properties of the coating are far from ideal. If the material does not melt, all the impact energy is dissipated through microstructural modifications such as recovery and recrystallization, leading to improvement of the overall properties. In this way, the microstructural behavior of the sprayed material strongly depends on the stress concentration at the particle–matrix interface, which is governed by the processing conditions employed during spraying. The plastic deformation increases as the particle velocity increases, governing the grain size related to dynamic recrystallization. The dynamic recrystallization effect is enhanced with increasing particle velocity and decreasing temperature. The grain size of the deposit increases as the gas temperature increases; unfortunately, increased gas temperature is necessary to increase the particle velocity. The presence of reinforcing particles play an important role in dynamic recrystallization, but with a different trend as a function of particle velocity compared with the base materials (Ref 23). Dynamic recrystallization takes place at low temperatures and high particle velocity; an increase in temperature under the same particle velocity conditions leads to a shift of the microstructural behavior toward shear instability and grain growth recorded after spraying.

The ceramic phase percentage has a strong effect on the adhesion strength. Figure 2 shows the variation of the adhesion strength as a function of the reinforcing phase percentage for NiCrAl-BN and Ti-$TiAl_3$. A decrease in the adhesion strength with increasing reinforcing percentage is exhibited for both materials. Ti-$TiAl_3$ exhibits very high levels of adhesion strength for $TiAl_3$ content of 5%. The adhesion strength values are much higher for Ti-$TiAl_3$ than for NiCrAl-BN. In fact, the mechanical properties of cold-sprayed coatings are strongly dependent on substrate–particle bonding, the level of which mainly depends on the differences in the mechanical properties of the particles and substrate. In the case of shear instability, the particle–substrate bonding is increased; this leads, in fact, to partial local melting induced by the deformation. This phenomenon can be controlled by appropriately tuning the gas temperature and pressure as a function of the particle and substrate properties (Ref 24, 25). When ceramic particles are present, a shift from cohesive to adhesive failure can be observed, potentially leading to a strong reduction in adhesion strength (Ref 26). Similar conclusions were reached by the authors of Ref 16 after wear tests.

The variation of the porosity as a function of the reinforcing phase percentage is shown in Fig. 3. The porosity decreases with increasing reinforcing phase percentage until reaching a minimum for both materials. This minimum is reached at around 30% BN for the NiCrAl-BN composite but at around 20% $TiAl_3$ for the Ti-$TiAl_3$ composite. After reaching this minimum level, the porosity starts to increase with further increase of the reinforcing phase percentage for both materials. A beneficial effect on the porosity is observed with increased reinforcement. The porosity decreases with increasing reinforcing particles in all the studied conditions up to 25% reinforcing particles. The porosity of the coating is directly related to the capability of the particles to flatten

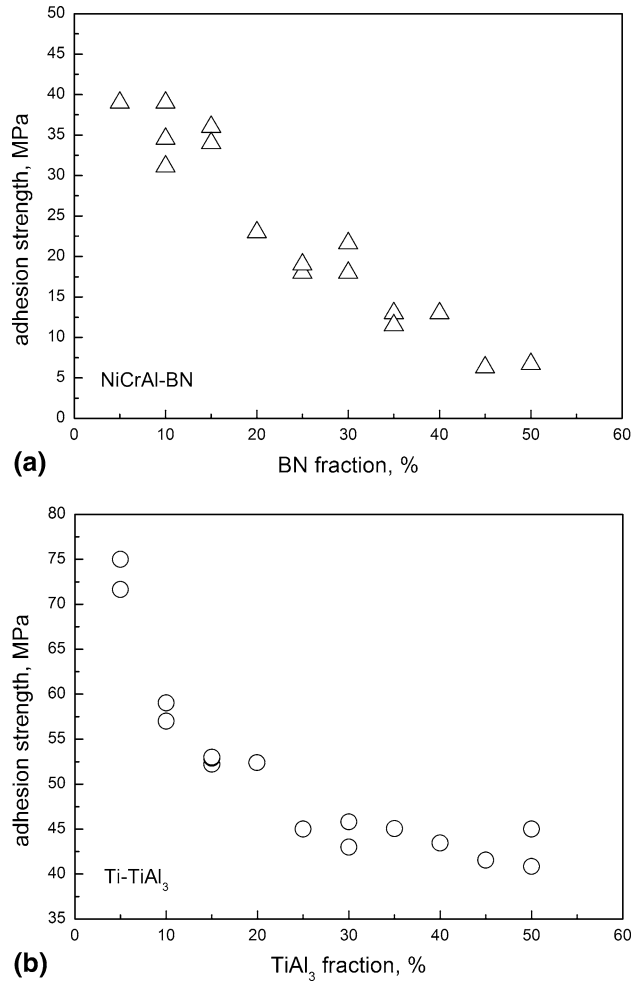

Fig. 2 Adhesion strength as a function of reinforcing phase percentage for NiCrAl-BN (a) and Ti-$TiAl_3$ (b)

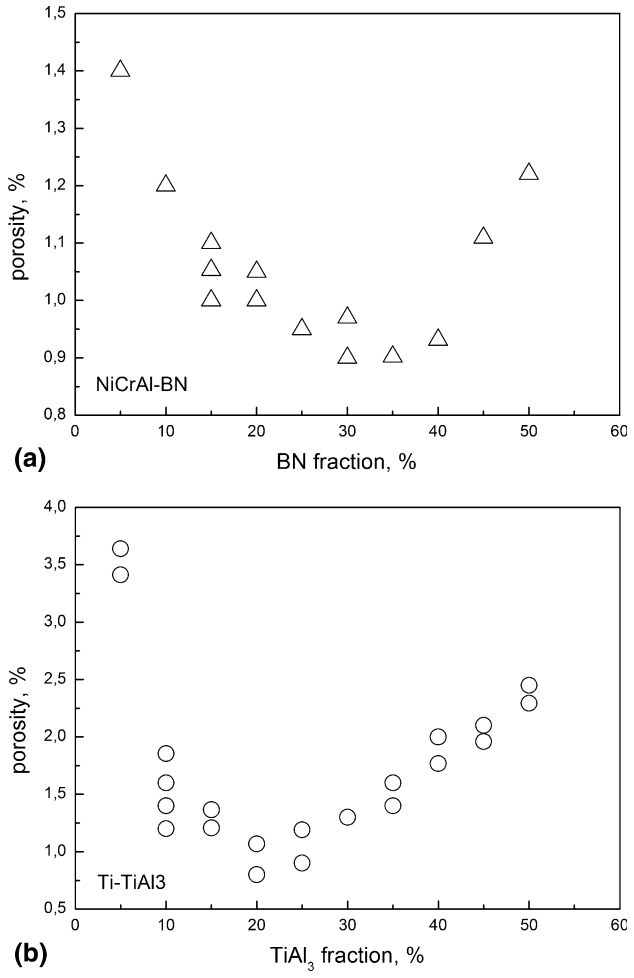

Fig. 3 Porosity variation as a function of reinforcing phase percentage for NiCrAl-BN (a) and Ti-$TiAl_3$ (b)

during impact, assuming a pancake-like shape with high aspect ratio. If the plastic deformation is insufficient, i.e., for nonoptimal processing parameter values, the particles do not reach the required aspect ratio, resulting in high porosity levels in the coating. In general, it can be affirmed that increase of the reinforcement percent increases the local plastic deformation (for the same velocity), leading to a decrease in the porosity (Ref 10).

The variation of the adhesion strength with the grain size dimensions in the deposit is shown in Fig. 4 for both materials. For comparison, the same is also plotted for the base materials (NiCrAl and Ti). For both materials, ceramic fractions in the range of 40–50% were employed. For the NiCrAl-BN composite, the adhesion strength was higher compared with the corresponding base metal. For the Ti-$TiAl_3$ composite, lower values of adhesion strength were registered with respect to pure Ti. For the NiCrAl-based materials, the adhesion strength increased with increasing grain size; for the Ti-based materials, the adhesion strength decreased with increasing grain size up to a point, and then started to increase with further increase of the grain size. In the case of titanium adhesion, the strength values exhibit a narrower range compared with the composite materials. This is due to the fact that the grain size variation in the cold-sprayed composites was narrower compared with the parent material, due to the strong grain refinement effect of the ceramic particles during spraying. The optimal particle velocity leads to high adhesion strength through increased particle temperature on impact and particle deformation. Various mechanisms take place during impact, influencing particle–substrate bonding. These include localized welding for impact fusion, diffusion, and metal–metal locking. The metal–metal locking and mechanical bonding are directly proportional to the particle velocity, while diffusion bonding increases with increasing impact temperature (Ref 27). In the case of metal–ceramic composites, bonding due to material melting reduces with increasing particle percentage. In such cases, in fact, recrystallization due to metal–ceramic interaction is the main mechanism involved during impact. The presence of ceramic particles reduces the overall temperature effect and phase transformations. The presence of ceramic particles, in addition, destroys oxide phases eventually deposited on the sub-

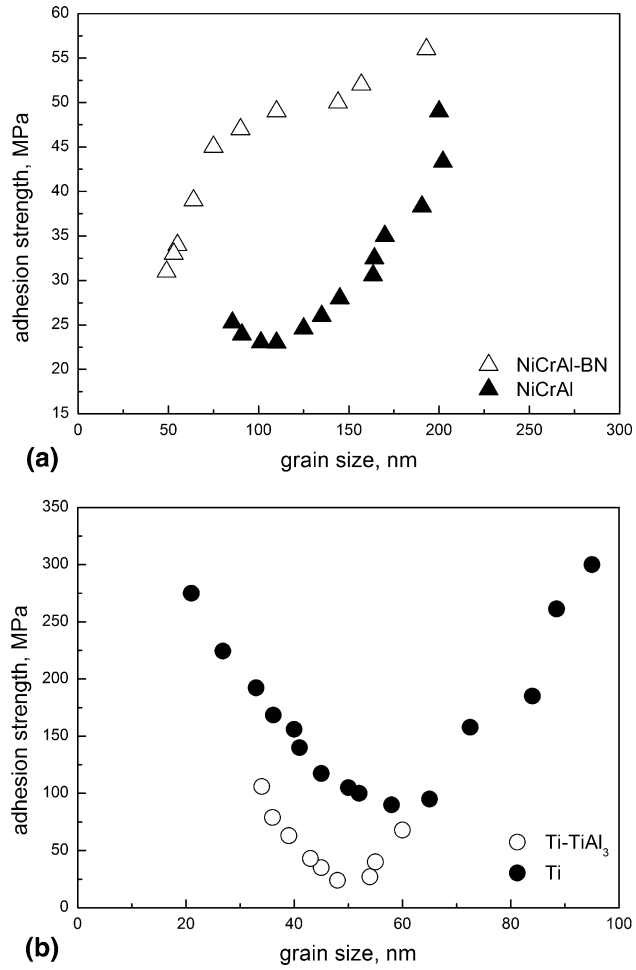

Fig. 4 Adhesion strength as a function of deposit grain size for NiCrAl-BN (a) and Ti-$TiAl_3$ (b) composites, compared with corresponding pure materials

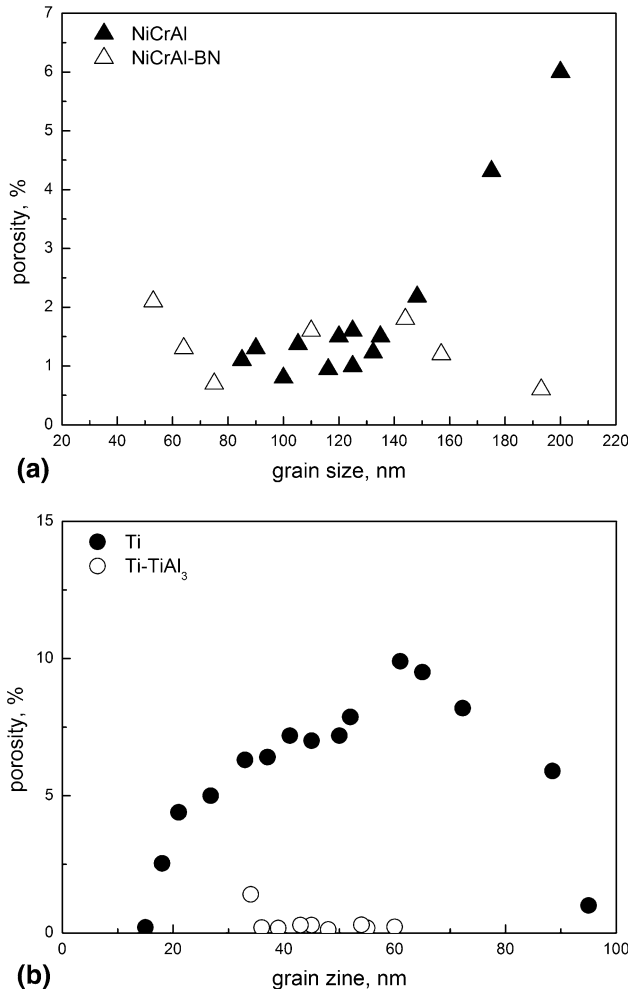

Fig. 5 Porosity variation as a function of grain size for NiCrAl-BN (a) and Ti-$TiAl_3$ (b) composites, compared with corresponding base materials

strate, thereby improving adhesion. Some authors also suggest that addition of ceramic particles creates additional microasperities, increasing the contact area.

The variation of the porosity as a function of the grain size of the deposit is shown in Fig. 5 for both materials. For comparison, the same is also plotted for the base materials (NiCrAl and Ti). The porosity increased with increasing grain size for NiCrAl, while it remained in a very narrow range for the NiCrAl-BN composite. The porosity in the Ti-$TiAl_3$ composite was always lower compared with the unreinforced material. It is clear from previous figures that the grain size is strongly influenced by the particle velocity; in particular, the grain size of the deposit decreases as the particle speed increases. In the case of cold-sprayed composites, this speed must be fixed in a narrower interval compared with the parent material, because (depending on the substrate hardness) hard particles can lead to undesirable cavitation and erosion phenomena (Ref 28). The variation of the microhardness of the studied composites as a function of particle speed and grain size is shown in Fig. 6. The Ti-$TiAl_3$ composite shows a continuous increase with increasing particle speed and decreasing grain size. The NiCrAl-BN composite shows a different behavior, exhibiting a continuous increase in hardness with particle speed up to 700 m/s, after which the microhardness increase shows a drop with further increase in particle speed.

The size and percentage of the particles in the matrix affect the adiabatic shear instability that governs recrystallization. Higher content and smaller dimensions of reinforcing particles result in a highly strain-hardened material due to the higher strain rates achieved during impact. In cold-sprayed composites, it is believed that the porosity depends on the capacity of the metallic phase to fill the gaps between the reinforcing particles. If the ductility of the material or the processing parameters employed are not sufficiently optimized, many small pores will be observed in the coating.

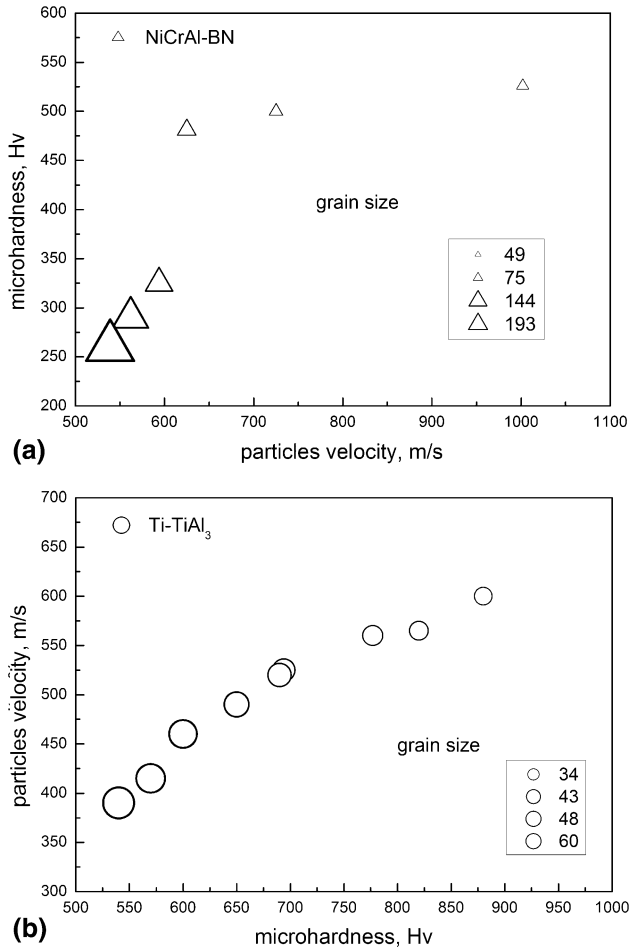

Fig. 6 Microhardness as a function of particle speed and grain size for NiCrAl-BN (a) and Ti-$TiAl_3$ (b) composites

4. Conclusions

The mechanical properties of Ti- and Ni-based metal–ceramic composites produced by cold spraying have been analyzed and described. Both materials exhibit a decrease in the grain size of the deposit with increasing particle velocity and reinforcing percentage. A decrease in the adhesion strength with increasing reinforcing percentage is shown by both materials. A beneficial effect on the porosity was observed with increasing reinforcement percentage. Different behavior was observed in comparison with the base materials. In particular, the reinforcing phase had a beneficial effect on the adhesion strength for the Ni-based composite, whereas the porosity was lower in unreinforced Ti with respect to the corresponding composite. The reinforcing material decreased the porosity for both composites compared with the unreinforced material.

References

1. P. Cavaliere, Cold Spray Coating Technology for Metallic Components Repairing, *Through-Life Engineering Services: Motivation Theory and Practice*, L. Redding and R. Roy, Ed., Springer, London, 2015, p 175-184 doi:10.1007/978-3-319-12111-6_11
2. O. Nooririnah, A.Y. Khalil, M.S. Aludin, A. Rohana, and R.R. Zuraidah, Overview Potential Applications of Cold Spray Process for Aviation Industry in Malaysia, *Adv. Mater. Res.*, 2013, **701**, p 375-377
3. R. Jones, M. Krishnapillai, K. Cairns, and N. Matthews, Application of Infrared Thermography to Study Crack Growth and Fatigue Life Extension Procedures, *Fat. Fract. Eng. Mater. Struct.*, 2010, **33**(12), p 871-884
4. A. Sova, D. Pervushin, and I. Smurov, Development of Multimaterial Coatings by Cold Spray and Gas Detonation Spraying, *Surf. Coat. Technol.*, 2010, **205**, p 1108-1114
5. M. Yandouzi, H. Bu, M. Brochu, and B. Jodoin, Nanostructured Al-Based Metal Matrix Composite Coating Production by Pulsed Gas Dynamic Spraying Process, *J. Therm. Spray Technol.*, 2012, **21**(3-4), p 609-619
6. R. Arrabal, A. Pardo, M.C. Merino, M. Mohedano, P. Casajús, and E. Matykina, Corrosion of Magnesium-Aluminum Alloys with Al-11Si/SiC Thermal Spray Composite Coatings in Chloride Solution, *J. Therm. Spray Technol.*, 2011, **20**(3), p 569-579
7. L. Kong, L. Bin, X. Cui, D. Hao, T. Li, and T. Xiong, Oxidation Behavior of $TiAl_3$/Al Composite Coating on Orthorhombic-Ti2AlNb Based Alloy at Different Temperatures, *J. Therm. Spray Technol.*, 2010, **19**(3), p 650-656
8. P. Cavaliere, A. Perrone, and A. Silvello, Processing Conditions Affecting Grain Size and Mechanical Properties in Nanocomposites Produced via Cold Spray, *J. Therm. Spray Technol.*, 2014, **23**(7), p 1089-1096
9. S.M. Hassani-Gangaraj, A. Moridi, and M. Guagliano, Critical Review of Corrosion Protection by Cold Spray Coatings, *Surf. Eng.*, 2014, doi:10.1179/1743294415Y.0000000018
10. A.S.M. Ang, C.C. Berndt, and P. Cheang, Deposition Effects of WC Particle Size on Cold Sprayed WC-Co Coatings, *Surf. Coat. Technol.*, 2011, **205**, p 3260-3267
11. R.S. Lima, J. Karthikeyan, C.M. Kay, J. Lindemann, and C.C. Berndt, Microstructural Characteristics of Cold-Sprayed Nanostructured WC-Co Coatings, *Thin Solid Films*, 2002, **416**, p 129-135
12. H.-K. Kang and S.B. Kang, Tungsten/Copper Composite Deposits Produced by a Cold Spray, *Scripta Mater.*, 2003, **49**, p 1169-1174
13. P.S. Phani, V. Vishnukanthan, and G. Sundararajan, Effect of Heat Treatment on Properties of Cold Sprayed Nanocrystalline Copper Alumina Coatings, *Acta Mater.*, 2007, **55**, p 4741-4751
14. X.-T. Luo and C.-J. Li, Thermal Stability of Microstructure and Hardness of Cold-Sprayed cBN/NiCrAl Nanocomposite Coating, *J. Therm. Spray Technol.*, 2012, **21**(3-4), p 578-585
15. X.-T. Luo, G-J. Yang, and C.-J. Li, Multiple Strengthening Mechanisms of Cold-Sprayed cBNp/NiCrAl Composite Coating, *Surf. Coat. Technol.*, 2011, **205**, p 4808-4813
16. X.-T. Luo, E.-J. Yang, F.-L. Shang, G.-J. Yang, C.-X. Li, and C.-J. Li, Microstructure, Mechanical Properties, and Two-Body Abrasive Wear Behavior of Cold-Sprayed 20 vol.% Cubic BN-NiCrAl Nanocomposite Coating, *J. Therm. Spray Technol.*, 2014, **23**(7), p 1181-1190
17. M. Grujicic, C.L. Zhao, W.S. De Rosset, and D. Helfritch, Analyses of the Impact Velocity of Powder Particles in the Cold-Gas Dynamic-Spray Process, *Mater. Sci. Eng. A*, 2004, **368**, p 222-230
18. M. Bashirzadeh, F. Azarmi, C.P. Leither, and G. Karami, Investigation on Relationship Between Mechanical Properties and Microstructural Characteristics of Metal Matrix Composites Fabricated by Cold Spraying Technique, *Appl. Surf. Sci.*, 2013, **275**, p 208-216
19. ASTM C633-13, Standard Test Method for Adhesion or Cohesion Strength of Thermal Spray Coatings, Book of Standards Volume: 02.05
20. S.R. Bakshi, V. Singh, K. Balani, D.G. McCartney, S. Seal, and A. Agarwal, Carbon Nanotube Reinforced Aluminum Composite Coating via Cold Spraying, *Surf. Coat. Technol.*, 2008, **202**, p 5162-5169
21. M. Grujicic, C.L. Zhao, W.S. DeRosset, and D. Helfritch, Adiabatic Shear Instability Based Mechanism for Particle/Substrate Bonding in the Cold-Gas Dynamic-Spray Process, *Mater. Des.*, 2004, **25**, p 681-688

22. T. Yang, M. Yu, H. Chen, W.Y. Li, and H.L. Liao, Characterisation of Cold Sprayed Al5056/SiCp Coating: Effect of SiC Particle Size, *Surf. Eng.*, 2015, doi:10.1179/1743294415Y.0000000042
23. T. Yang, M. Yu, H. Chen, W.Y. Li, and H.L. Liao, Effect of Matrix/Reinforcement Combination on Cold Sprayed Coating Deposition Behavior, *Surf. Eng.*, 2014, **30**(11), p 796-800
24. T. Hussain, Cold Spraying of Titanium: A Review of Bonding Mechanisms, Microstructure and Properties, *Key Eng. Mater.*, 2013, **533**, p 53-90
25. G. Bae, J.I. Jang, and C. Lee, Correlation of Particle Impact Conditions with Bonding, Nanocrystal Formation and Mechanical Properties in Kinetic Sprayed Nickel, *Acta Mater.*, 2012, **60**(8), p 3524-3535
26. M. Yandouzi, L. Ajdelsztajn, and B. Jodoin, WC-Based Composite Coatings Prepared by the Pulsed Gas Dynamic Spraying Process: Effect of the Feedstock Powders, *Surf. Coat. Technol.*, 2008, **202**, p 3866-3877
27. O. Meydanoglu, B. Jodoin, and E.S. Kayali, Microstructure, Mechanical Properties and Corrosion Performance of 7075 Al Matrix Ceramic Particle Reinforced Composite Coatings Produced by the Cold Gas Dynamic Spraying Process, *Surf. Coat. Technol.*, 2013, doi:10.1016/j.surfcoat.2013.07.020
28. H.X. Hu, S.L. Jiang, Y.S. Tao, T.Y. Xiong, and Y.G. Zheng, Cavitation Erosion and Jet Impingement Erosion Mechanism of Cold Sprayed Ni-Al_2O_3 Coating, *Nucl. Eng. Des.*, 2011, **241**, p 4929-4937